Journal of Chromatography A 1665 (2022) 462832

Contents lists available at ScienceDirect

Journal of Chromatography A

journal homepage: www.elsevier.com/locate/chroma

Ultrahigh-performance supercritical fluid chromatography – mass spectrometry for the qualitative analysis of metabolites covering a large polarity range

Michela Antonelli, Michal Holčapek, Denise Wolrab*

Department of Analytical Chemistry, Faculty of Chemical Technology, University of Pardubice, Studentská 573, Pardubice 53210, Czech Republic

ARTICLE INFO

Article history:
Received 9 December 2021
Revised 13 January 2022
Accepted 13 January 2022
Available online 15 January 2022

Keywords:
Supercritical fluid chromatography
Metabolites
Amino acids
Human plasma
Mass spectrometry

ABSTRACT

The applicability of ultrahigh-performance supercritical fluid chromatography coupled with mass spectrometry (UHPSFC/MS) for the qualitative analysis of metabolites with a wide polarity range (log P: −3.89–18.95) was evaluated using a representative set of 78 standards belonging to nucleosides, biogenic amines, carbohydrates, amino acids, and lipids. The effects of the gradient shape and the percentage of water (1, 2, and 5%) were investigated on the Viridis BEH column. The screening of eight stationary phases was performed for columns with different interaction sites, such as hydrogen bonding, hydrophobic, π-π, or anionic exchange type interactions. The highest number of compounds (67) of the set studied was detected on the Torus Diol column, which provided a resolution parameter of 39. The DEA column had the second best performance with 58 detected standards and the resolution parameter of 54. The overall performance of other parameters, such as selectivity, peak height, peak area, retention time stability, asymmetry factor, and mass accuracy, led to the selection of the Diol column for the final method. The comparison of additives showed that ammonium acetate gave a superior sensitivity over ammonium formate. Moreover, the influence of the ion source on the ionization efficiency was studied by employing atmospheric pressure chemical ionization (APCI) and electrospray ionization (ESI). The results proved the complementarity of both ionization techniques, but also the superior ionization capacity of the ESI source in the negative ion mode, for which 53% of the analytes were detected compared to only 7% for the APCI source. Finally, optimized analytical conditions were applied to the analysis of a pooled human plasma sample. 44 compounds from the preselected set were detected in human plasma using ESI-UHPSFC/MS in MS^E mode considering both ionization modes.

© 2022 The Authors. Published by Elsevier B.V.
This is an open access article under the CC BY-NC-ND license (http://creativecommons.org/licenses/by-nc-nd/4.0/)

1. Introduction

Metabolomics can be described as the comprehensive study of small molecules, called metabolites, in the organism and the association of those with pathophysiological states [1,2]. Metabolomic analysis requires the use of highly powerful analytical techniques, such as mass spectrometry (MS) hyphenated to chromatographic separation techniques, such as liquid chromatography (LC) or gas chromatography, as a means to simultaneously analyze complex mixtures of metabolites [3]. The most widespread separation modes used for metabolomics are reversed-phase ultrahigh-performance liquid chromatography (RP-UHPLC) and hydrophilic interaction liquid chromatography (HILIC-UHPLC) coupled to high-resolution (HR) MS instruments, such as quadrupole-time-of-flight (QTOF) or Orbitrap [4]. The comprehensive analysis of the metabolome is challenging due to the high chemical and structural diversity of metabolites. In RP-UHPLC, intermolecular hydrophobic interactions between analytes, stationary phase, and mobile phase allow analysis of a large part of the metabolome of complex biological samples such as urine, plasma, and tissue extracts [5–7]. However, polar and/or ionic species are poorly retained in RP-UHPLC [8]. The retention mechanism in the HILIC mode is based on the interaction of polar analytes with the polar stationary phase, which allows the separation of the analytes. Therefore, HILIC provides complementary chromatographic separation compared to RP-UHPLC/MS [9,10]. Nonpolar compounds may elute in or close to the void volume in HILIC mode. A comprehensive technique that allows the separation of polar and non-polar metabolites, such as lipids, amino acids, and nucleosides, is desired.

* Corresponding author.
E-mail address: denise.wolrab@upce.cz (D. Wolrab).

https://doi.org/10.1016/j.chroma.2022.462832
0021-9673/© 2022 The Authors. Published by Elsevier B.V. This is an open access article under the CC BY-NC-ND license (http://creativecommons.org/licenses/by-nc-nd/4.0/)

Recently, UHPSFC gained attention, because the new generation instruments allow stable and reproducible results as well as routine hyphenation to mass spectrometry [11,12]. Mainly, the backpressure regulator, injector, and column technology were improved for the new generation instruments, leading to better acceptance of UHPSFC/MS for a broad application range. Generally, the use of supercritical fluid chromatography (SFC) was first described more than 50 years ago [13], but its application for lipidomic [14,15] and metabolomic analysis [12,16,17] represents a rather recent trend. UHPSFC may represent a potential alternative to RP- and HILIC-UHPLC for the comprehensive analysis of the metabolome by reducing the costs and analysis time. Nowadays, UHPSFC mainly uses supercritical CO_2 mixed with organic modifiers as the mobile phase. The addition of organic solvents, typically 2–40%, broadens the range of analytes that can be separated with UHPSFC. Polar solvents, such as methanol, ethanol, or acetonitrile, are the most commonly used and facilitate the elution of polar compounds. The addition of small percentages of water, salts, bases, and/or acid additives to the modifier can further improve the peak shape and the elution of polar and ionic compounds [18–20]. The low viscosity and high diffusion of the mobile phase in UHPSFC allow the use of high flow rates without losing separation efficiency and therefore allow high-throughput analyzes [21,22]. Furthermore, almost all stationary phases used for UHPLC can also be used for UHPSFC including modern stationary phases packed with sub-3 µm core shell and fully porous particles [23–26]. Recently, dedicated UHPSFC stationary phases were also introduced to the market, such as the Torus column series from Waters. These stationary phases are based on silica modified with different selectors, such as propanediol, 1-aminoanthracene, diethylamine, 2-picolylamine, or ethylene-bridged silica, which are potentially suitable for the separation of medium to polar metabolites [18,21,27]. It should be mentioned that the analysis of very polar compounds still remains challenging for UHPSFC/MS employing common chromatographic conditions. The increase in the percentage of modifier in CO_2 up to 100% during the gradient increases the elution strength for polar compounds and extends the polarity range of analytes suitable for the separation with UHPSFC/MS instruments. These special modes using increased modifier and CO_2 as the mobile phase are called unified chromatography or enhanced fluid chromatography [20,28]. However, such mobile phase conditions and the use of sub-2 µm particle columns can lead to exceeding system pressure forcing adjustment of parameters, such as backpressure, temperature, or flow rate. Consequently, the analyzes may be performed by increasing the organic solvent in the mobile phase gradient and, at the same time, decreasing the flow rates. Following this approach in metabolomics and using a polar stationary phase, the elution ranges from nonpolar to polar compounds [12].

In recent years, more UHPSFC/MS applications have been investigated, accompanied by unconventional and innovative developments regarding the applied conditions and instrumental settings. Analysis of natural products, biological samples [29–32], pharmaceuticals, nutrients, and environmental samples are examples for the application areas of UHPSFC [33]. However, only a few studies investigated metabolomics by UHPSFC/MS. The potential of UHPSFC/MS for the analysis of polar urinary metabolites was investigated by Sen et al., who evaluated 12 different columns, 3 column temperatures, and 9 different additives in methanol, for the separation of 60 polar metabolites (log P −7 to 2) [18]. *Desfontaine* et al. described the application of UHPSFC coupled to a triple-quadrupole MS for the analysis of nucleosides, small bases, lipids, small organic acids, and sulfated metabolites [12]. The analytical method was optimized by investigating several parameters such as the kinetic performance, the percentage of cosolvent, the type of stationary phase, and the composition of the mobile phase. Additionally, the mixture of 57 compounds was also analyzed by unified chromatography coupled with MS. Losacco et al. analyzed 49 metabolites in plasma and urine using UHPSFC/QTOF-MS with the evaluation of the impact of the biological matrix. Most of selected compounds were not affected by matrix interference (63%), whereby 16% of compounds showed a matrix effect in urine and plasma samples [16]. The UHPSFC/MS analysis of free amino acids was investigated by Raimbault et al. [20]. The separation of 18 native proteinogenic amino acids was achieved by applying unified chromatographic conditions, starting from 90% CO_2 to 100% modifier.

The aim of this work was to evaluate the suitability of UHPSFC/MS for the analysis of 78 metabolites selected from the Human Metabolome Database (HMDB) database based on their relevance in cancer research. To achieve the elution of all analytes, enhanced fluid chromatography was applied because the analyte set covers a wide polarity range (log P: −3.89 – 18.95). The influence of the percentage of water in the modifier, the gradient shape, and the type of stationary phase for the separation of the analyte set was evaluated using UHPSFC/QTOF-MS. The ionization efficiency of the selected metabolites employing electrospray ionization (ESI) and atmospheric pressure chemical ionization (APCI) was compared. The MS^E mode was applied for the analysis of the standard metabolite mixture and plasma samples.

2. Materials and methods

2.1. Chemicals

Methanol (CH_3OH), acetonitrile (ACN), 2-isopropanol, hexane (all LC/MS gradient grade), water (H_2O; LC/MS Ultra, UHPLC/MS grade), and chloroform (LC grade, stabilized with 0.5–1% ethanol) were purchased from Honeywell (Charlotte, North Caroline, US). Ammonium acetate, ammonium formate (LC/MS, gradient grade), and formic acid (98–100%, Suprapur) were purchased from Sigma-Aldrich or Merck (St. Louis, MO, U.S.A), respectively. Carbon dioxide (CO_2) 4.5 grade (99.995%) was obtained from Messer Group GmbH (Bad Soden, Germany).

2.2. Standards

The standards were purchased from Sigma-Aldrich (see Table 1). Standard stock solutions were prepared by dissolving each compound in the appropriate solvent or solvent mixture (Table S1) to obtain the final concentration of 10 mg mL^{-1}. Afterwards, nine standard mixtures were prepared according to the analyte category and diluted in MeOH, that is, mixtures of nucleosides (N°1; 100 ng μL^{-1}), biogenic amines (N°2; 20–100 ng μL^{-1}), sugars together with other organic compounds (N°3; 100–10 ng μL^{-1}), amino acids (N°4–8; 2–100 ng μL^{-1}) and lipids (N°9; 10 ng μL^{-1}). Analytes in each mixture are reported in Table S1. Standard concentrations in the final mixture were established by investigating the efficiency and sensitivity of ionization using direct infusion MS for 10 ng μL^{-1} and 100 ng μL^{-1} as well as two different sample solvent solutions, MeOH and MeOH/ACN (50:50, *v/v*). The optimized source parameters, standard concentration, and sample solvent were used for further experiments. These standard mixtures (100 µL of each) and guanine (10 µL) were mixed, and the final standard solution was diluted with acetonitrile to obtain a final solvent composition of CH_3OH/ACN (50:50, *v/v*) for UHPSFC/MS analyzes (Table S1).

2.3. Stationary phases

The final standard solution was analyzed using eight different columns, reported in Table 2. The stationary phases differ in their column chemistry, providing different interaction sites and

Table 1
List of standard compounds.

Compounds	Molecular formula	Exact Mass	$Log_{10}P$
Nucleosides			
Adenosine	$C_{10}H_{13}N_5O_4$	267.0967	−1.05
2-Deoxyadenosine	$C_{10}H_{13}N_5O_3$	251.1018	−0.55
Adenine	$C_5H_5N_5$	135.0545	0
Uridine			
	$C_9H_{12}N_2O_6$	244.0695	−2.28
Guanosine	$C_{10}H_{13}N_5O_5$	283.0917	−2.76
Guanine	$C_5H_5N_5O$	151.0494	−1.27
Xanthosine	$C_{10}H_{12}N_4O_6$	284.0757	−1.26
Biogenic amines			
Putrescine	$C_4H_{12}N_2$	88.1000	−0.99
Spermidine	$C_7H_{19}N_3$	145.1579	−1.26
Spermine	$C_{10}H_{26}N_4$	202.2157	−0.5
Adrenaline	$C_9H_{13}NO_3$	183.0895	−1.37
Noradrenaline	$C_8H_{11}NO_3$	169.0739	−0.24
Dopamine	$C_8H_{11}NO_2$	153.079	0.58
Serotonin	$C_{10}H_{12}N_2O$	176.095	0.51
Histamine	$C_5H_9N_3$	111.0796	−1.09
Tryptamine	$C_{10}H_{12}N_2$	160.1000	0.9
N-acetyl-5-hydroxytryptamine	$C_{12}H_{14}N_2O_2$	218.1055	0.44
Melatonin	$C_{13}H_{16}N_2O_2$	232.1212	0.71
Octopamine hydrochloride	$C_8H_{11}NO_2$	153.079	−0.9
Amino acids			
L-Alanine	$C_3H_7NO_2$	89.0477	−2.85
L-Threonine	$C_4H_9NO_3$	119.0582	−1.43
L-Leucine	$C_6H_{13}NO_2$	131.0946	−1.62
L-Norleucine	$C_6H_{13}NO_3$	131.0946	0.43
L-Isoleucine	$C_6H_{13}NO_4$	131.0946	−1.70
L-Arginine	$C_6H_{14}N_4O_2$	174.1117	−3.5
Glutamic acid	$C_5H_9NO_4$	147.0531	−1.39
L-Glutamine	$C_5H_{10}N_2O_3$	146.0691	−2.05
L-Histidine monohydrochloride	$C_6H_9N_3O_2$	155.0695	−1.67
L-Methionine	$C_5H_{11}NO_2S$	149.051	−0.56
Ornithine	$C_5H_{12}N_2O_2$	132.0899	−1.57
Phenylalanine	$C_9H_{11}NO_2$	165.0788	−1.49
Serine	$C_3H_7NO_3$	105.0426	−1.75
L-Carnitine	$C_7H_{15}NO_3$	161.1052	−2.9
Valine	$C_5H_{11}NO_2$	117.079	−0.01
L-Tyrosine	$C_9H_{11}NO_3$	181.0739	−2.15
L-Tryptophan	$C_{11}H_{12}N_2O_2$	204.0899	−1.07
1-Methyl-L-Tryptophan	$C_{12}H_{14}N_2O_2$	218.1055	0.84
5-Hydroxy-L-Tryptophan	$C_{11}H_{12}N_2O_3$	220.0848	−0.07
L-Proline	$C_5H_9NO_2$	115.0633	−0.4
D,L-Asparagine	$C_4H_8N_2O_3$	132.0535	−2.33
L-Lysine	$C_6H_{14}N_2O_2$	146.1055	−1.15
Taurine	$C_2H_7NO_3S$	125.0147	−1.72
Aspartic acid	$C_4H_7NO_4$	133.0375	−3.89
Acetyl-L-carnitine hydrochloride	$C_9H_{17}NO_4$	203.1157	−0.66
D,L-Octanoylcarnitine chloride	$C_{15}H_{29}NO_4$	287.2096	1.68
D,L-Decanoylcarnitine chloride	$C_{17}H_{33}NO_4$	315.2409	2.46
D,L-Lauroylcarnitine chloride	$C_{19}H_{37}NO_4$	343.2722	3.24
D,L-Myristoylcarnitine chloride	$C_{21}H_{41}NO_4$	371.3035	4.02
D,L-Palmitoylcarnitine chloride			
	$C_{23}H_{45}NO_4$	399.3348	4.8
Sugars			
D-Glucose	$C_6H_{12}O_6$	180.0634	−3.24
D-Xylose	$C_5H_{10}O_5$	150.0528	−2.71
Myo-inositol	$C_6H_{12}O_6$	180.0634	−3.22
Other organic compounds			
Caffeine	$C_8H_{10}N_4O_2$	194.0804	−0.8
Folic acid	$C_{19}H_{19}N_7O_6$	441.1397	−0.04
5-Methoxyindole	C_9H_9NO	147.0684	1.45
5-Hydroxyindole	C_8H_7NO	133.0528	1.19
D,L-Kynurenine	$C_{10}H_{12}N_2O_3$	208.0448	−0.82
Polar lipids			
PC (18:1/18:1)	$C_{44}H_{84}NO_8P$	785.5934	13.15
LPC (18:1/0:0)	$C_{26}H_{52}NO_7P$	521.3481	6.56
PE (18:1/18:1)	$C_{41}H_{78}NO_8P$	743.5465	13.2
LPE (18:1/0:0)	$C_{23}H_{48}NO_7P$	479.3012	6.62
PS (16:0/18:1)	$C_{40}H_{76}NO_{10}P$	761.5207	12.1
LPS (18:1/0:0)	$C_{24}H_{46}NO_9P$	523.291	6.07
PG (18:1/18:1)	$C_{42}H_{79}O_{10}P$	774.5411	12.89
LPG (18:1/0:0)	$C_{24}H_{47}O_9P$	510.2958	3.97
PA (18:1/18:1)	$C_{39}H_{73}O_8P$	700.5043	12.82

(*continued on next page*)

Table 1 (*continued*)

Compounds	Molecular formula	Exact Mass	$Log_{10}P$
LPA (18:1/0:0)	$C_{21}H_{41}O_7P$	436.259	4.69
GalCer (d18:1/12:0)	$C_{36}H_{69}NO_8$	643.5023	8.4
LacCer (d18:1/16:0)	$C_{46}H_{87}NO_{13}$	861.6177	5.81
Cer (d18:1/18:1)	$C_{36}H_{69}NO_3$	563.5277	10.98
Mono-Sulfo-GalCer(d18:1/24:1)	$C_{48}H_{91}NO_{11}S$	889.6313	13.94
SM (d18:1/18:1)	$C_{41}H_{81}N_2O_6P$	728.5832	11.76
SPH d18:1 (sphingosine)	$C_{18}H_{37}NO_2$	299.2824	4.78
SPH d18:0 (sphinganine)	$C_{18}H_{39}NO_2$	301.2981	5.01
Nonpolar lipids			
MG (0:0/18:1/0:0)	$C_{21}H_{40}O_4$	356.2927	5.78
DG (18:1/0:0/18:1)	$C_{39}H_{72}O_5$	620.538	12.37
Prostaglandin E2	$C_{20}H_{32}O_5$	352.225	3.82
TG (18:1/18:1/18:1)	$C_{57}H_{104}O_6$	884.7833	18.95

Table 2
Columns screened in this study.

Column name	Support	Bonded ligand	Dimensions (mm)	Particle size (μm)
ACQUITY UPC^2 BEH	Fully porous hybrid silica	_	100 × 3.0	1.7
ACQUITY UPC^2 Torus Diol	Fully porous hybrid silica	Propanediol	100 × 3.0	1.7
ACQUITY UPC^2 Torus 2-PIC	Fully porous hybrid silica	2-Picolyl-amine	100 × 3.0	1.7
ACQUITY UPC^2 Torus 1AA	Fully porous hybrid silica	1-Amino-anthracene	100 × 3.0	1.7
ACQUITY UPC^2 Torus DEA	Fully porous hybrid silica	Diethylamine	100 × 3.0	1.7
ACQUITY UPC^2 HSS C18 SB	Fully porous silica	Octadecyl, nonendcapped	100 × 3.0	1.8
ACQUITY UPC^2 Trefoil CEL1	_	Modified polysaccharide	150 × 3.0	2.5
ACQUITY UPLC HSS T3	_	Octadecyl, endcapped	100 × 2.1	1.8

therefore may show different selectivities. The Viridis BEH column (100 × 3.0 mm I.D, 1.7 μm) was selected for the preliminary study. In addition, the Torus columns, namely, Diol, 2-PIC, 1-AA, and DEA (100 × 3.0 mm I.D, 1.7 μm), were evaluated. The diol and BEH columns represent the most polar stationary phases among the selected ones, characterized by propandiol - bonded silica support and free silanols, respectively. Furthermore, two columns packed with modified C18 silica were included for column screening, namely, HSS C18 SB column (100 × 3.0 mm, 1.8 μm) and HSS T3 (100 × 2.1 I.D; 1.8 μm). Additionally, the chiral stationary phase Trefoil CEL 1 (150 × 3.0 mm I.D; 2.5 μm) was tested. All columns were purchased from Waters (Milford, MA, USA).

2.4. UHPSFC/MS/MS instrumentation

UHPSFC/MS/MS analysis was performed on the Acquity UPC^2 (Waters, Milford, MA, USA) hyphenated with the Synapt G2-Si (Waters) QTOF mass spectrometer. The UHPSFC instrument was coupled to the MS using the commercial interface kit (Waters). Gradient mode was used for screening the stationary phase selected for the separation of the metabolite mixture. Supercritical carbon dioxide ($scCO_2$) was used as the mobile phase A, and MeOH with 30 mmol L^{-1} ammonium acetate and 1, 2, or 5% of H_2O or MeOH with 30 mM ammonium formate and 2% of H_2O was investigated as mobile phase B (modifier). The gradient started with 5% of B, was increased to 70% B in 8.5 min, then to 100% B in 10.5 min, kept constant for 2.5 min, and finally returned to the initial condition within 1 min and re-equilibrated for 1 min, with a total run time of 15 min. Furthermore, a flow gradient was employed to avoid instrument overpressure at 100% of the modifier; the starting flow was set to 2.0 mL min^{-1}, decreased to 0.8 mL min^{-1} within 14 min, and back to the initial flow in 1 min. The ABPR was set at 1800 psi and the column temperature at 60 °C. The injection volume was 1 μL, and the injection needle was washed after each injection with hexane/2-isopropanol/H_2O (2:2:1, *v/v/v*). MeOH with 0.1% of formic acid and 5% of H_2O was used as a make-up solvent to improve the ionization. Furthermore, a flow gradient for the make-up solvent was used: 0 min – 0.6 mL min^{-1}, 8.5 min – 0.2 mL min^{-1}, 13 min – 0.2 mL min^{-1}, 14 min – 0.6 mL min^{-1}, 15 min – 0.6 mL min^{-1}.

The following settings were used for QTOF measurements: HR mode, a mass range of *m/z* 50–950, and the continuum mode with a scan time of 0.1 s were applied. Leucine enkephalin was used as the lock mass, in which the lock mass was acquired with a scan time of 0.1 s in 10 s intervals, but no automatic lock mass correction was applied. ESI and APCI in positive and negative ion modes were investigated. The following parameters were used for the ESI mode: capillary voltage 2.50 kV, sampling cone 20 V, source offset 90 V, source temperature 150 °C, desolvation temperature 350 °C, cone gas flow 50 L/h, desolvation gas flow 1000 L/h and nebulizer gas flow 3.5 bar. The following parameters were used for the APCI mode: corona current 1.0 μA, sampling cone 10 V, cone gas flow 50 L/h, nebulizer gas flow 3.5 bar, source offset 50 V, source temperature 150 °C, probe temperature 600 °C and lock spray capillary voltage 3.0 kV. Column screening was performed in positive and negative ion mode using ESI and full scan spectra acquisition. Furthermore, the MS^E mode was applied to detect the MS spectra and the corresponding fragment spectra of each compound in one run. The MS^E method is characterized by two stages. In stage 1, all ions are transmitted from the ion source through the collision cell, wherein low collision energy is applied so that no fragmentation can be observed in the mass analyzer, and ions are recorded as the precursor ions. In stage 2, all ions are transmitted from the ion source through the collision cell, and a collision energy ramp is applied to generate and record fragment ions in the mass analyzer. Hence, the software is able to generate two spectra at the same time; the first one shows the precursor ions with no collision energy, and the second one generates fragment ions due to the applied collision energy. The trap and transfer collision energy of the low energy function was kept off and the ramp trap collision energy of the high energy function was set from 5 to 30 V. – The obtained fragments were compared with online databases, i.e., HMDB and MzCloud for further confirmation.

2.5. Biological sample preparation

Human plasma collected from different healthy volunteers was pooled, worked up, and analyzed with UHPSFC/MS under optimized conditions. All subjects signed an informed consent. An additional step, namely, limited digestion with proteinase K was added. Before protein precipitation, 2 µL of Proteinase K and 2 µL of 250 mM $CaCl_2$ were added to 100 µL of plasma sample to obtain a final concentration of 5 mM and sonicated for 15 min at 40 °C. For protein precipitation, 1 mL of CH_3OH/EtOH (1:1, *v/v*) was added to the pooled plasma sample sonicated for 15 min at room temperature (25 °C) and stored for 1 h at −20 °C. The sample was centrifuged for 15 min at 10,000 rpm, the supernatant was transferred to a glass vial and evaporated under nitrogen. The residue was dissolved with 35 µL of ACN/CH_3OH/H_2O (4:4:2, *v/v/v*) + 0.1% formic acid and diluted 1:10 with the same solvent mixture. 1 µL was injected for the subsequent UHPSFC/MS analysis.

2.6. Data processing

Data were acquired with the MassLynx software (Waters). The Waters Compression Tool was used for noise reduction, which also minimized the raw data file size facilitating data handling. The Accurate Mass Measure tool in MassLynx was used to apply lock mass correction for better mass accuracy and for the conversion of data from continuum to centroid mode, which further reduced the file size. Finally, TargetLynx was used to extract retention times, peak areas, peak height, peak widths (Pk width), and asymmetry factors by providing exact masses and expected retention times of all compounds. The resulting tables were exported as .csv files and further processed with Microsoft Excel, i.e., to calculate the number of identified standards and the relative standard deviation (RSD%) of the retention time, peak area and peak height. MarkerLynx was used to generate feature lists of *m/z* with the corresponding retention time, which allowed the calculation of the mass accuracy. The complete summary tables from MarkerLynx were exported as .csv files and manually checked for experimental *m/z* of each standard or target analyte.

Furthermore, MZmine 2.53 software [34] software was used to assess the influence of the data processing procedure. The following settings were applied: the targeted peak detection module was used to search the list of compounds with a precursor mass tolerance of 0.002 *m/z* or 5 ppm and a retention time tolerance of 0.1 min. Peak integration was checked and manually corrected when needed. Retention times, peak areas, peak heights, peak widths (FWHM), asymmetry factors, and experimental *m/z* were exported as .csv files and further processed with Microsoft Excel. For the chromatographic evaluation, the resolution and selectivity (α) were calculated. The results of two different software solutions were compared (Tables 3 and S11).

MSDIAL ver. 4.70, was used for metabolite identification in real human plasma using the databases MSMS-Public-pos-VS15 for positive and MSMS-Public-Neg-VS15 for negative ion mode. The databases are composed of metabolites in plasma, which were detected by the MSDIAL community, whereby 13,303 entries are included for positive ion mode and 12,879 entries for negative ion mode.

3. Results and discussion

3.1. Selection of standard compounds

The selected analytes (Tables 1 and S1) were selected from the Human Metabolome Database based on their biological relevance with a special focus on the metabolites involved in cancer progression [12,16]. The final metabolite mixture varied in molecular weights from 89 to 900 Da and log10P values from −3.89 to 18.95 (Fig. 1). The substantial variety in the structural composition and chemical characteristics of selected compounds, i.e., polar amino acids to hydrophobic lipids such as triacylglycerols, leads to highly diverse retention time behavior and different ionization efficiencies, altering sensitivity. The list includes metabolites involved in various biological pathways, e.g., metabolites derived from the tryptophan pathway. Tryptophan is an essential amino acid, a building block for protein biosynthesis and functions as a precursor for the conversion to several other metabolites included in our list, i.e., 5-hydroxytryptophan, tryptamine, serotonin, melatonin, N-acetyl-5-hydroxytryptamine, L-kynurenine, L-alanine, and glutamic acid. Furthermore, clinical studies have shown that tryptophan metabolism promotes tumor progression through multiple mechanisms [35], and its metabolic derivative L-kynurenine is involved in Alzheimer's disease and the early stages of Huntington's disease. The catecholamines dopamine, adrenaline, and noradrenaline are derived from the tyrosine pathway [36] with an implication in the treatment of dopamine-responsive dystonia and Parkinson's disease. In general, biogenic amines and amino acids were chosen for their importance in several types of cancer, namely, ovarian, breast, pancreatic, colon, and oral cancers, and neurodegenerative diseases. Similarly, sugars were included in this optimization due to their large consumption by tumor cells [37]. Other two important biological classes of compounds are nucleosides and lipids, for which evident changes have been observed in cancer patients [38,39]. The involvement of lipids in different types of tumors such as pancreatic, gastric, liver, lung, colorectal, and thyroid cancer was shown [40]. A schematic overview of the biosynthesis reactions is presented in the supplementary information (Figs. S1 and S2), clearly illustrating how the various analytes are interrelated. In total 64 from the 78 analytes shown, the missing 14 analytes mainly include metabolites, which are uptaken by dietary means such as essential amino acids (6), caffeine and folic acid, and consequently no biosynthesis can be shown. The remaining analytes were included in the analyte set for mechanistic questions, i.e., isomers. The importance and connection of amino acids for the biosynthesis of biogenic amines, glucose as well as lipids can be seen. Further, it is commonly assumed that the dysregulation or absence of some metabolites may harm the well-being.

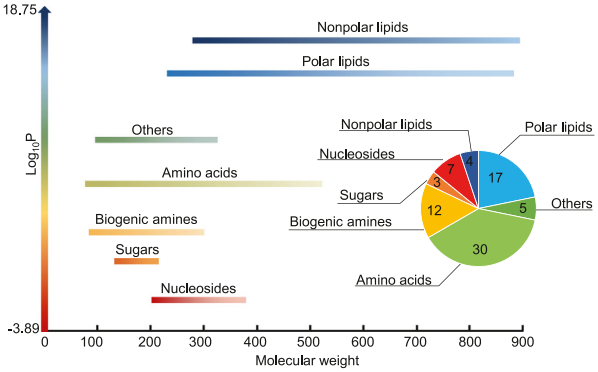

Fig. 1. Relation of partition coefficients ($log_{10}P$) and molecular weights for the investigated analytes and the number of metabolites categorized by compound class: nucleosides (red), biogenic amine (yellow), amino acids (green), sugars (orange), others (dark green), polar lipids (light blue), and nonpolar lipids (blue).

To facilitate the elution of non-polar, polar, and ionic metabolites, the addition of methanol, including additives, to $scCO_2$ was necessary. A small amount of water was added to the mobile phase to improve the peak shape and solvation of polar analytes. As a consequence of the limited maximum upper pressure of the UHPSFC system, it was not possible to maintain high flow rates and reach 100% of the modifier for the elution of polar compounds

Table 3
Summary tables of mass accuracy, selectivity, resolution, and the repeatability of the retention time, signal area, and signal height calculated by the average RSD% for ammonium acetate and ammonium formate in positive and negative ionization mode using TargetLynx and MZmine as data processing software.

TargetLynx	Ammonium acetate positive	Ammonium Formate negative	positive	negative
Mass Accuracy (ppm)	2.94	2.81	1.64	1.64
Selectivity	2.36	1.3	6.57	1.32
Resolution	39	36	40	39
Repeatability (RSD%)				
Retention time	0.2	0.15	0.52	0.1
Signal Area	8.95	7.84	7.17	9.28
Signal Height	9.26	8.33	7.45	10.09
MZmine				
Mass Accuracy (ppm)	2.78	1.98	2.32	2.1
Selectivity	2.35	1.28	7.28	1.06
Resolution	35	29	36	20
Repeatability (RSD%)				
Retention time	0.31	0.13	0.61	0.14
Signal Area	14.56	10.29	11.6	12.31
Signal Height	10.06	7.57	9.29	10.57

at the same time. Therefore, a decreasing flow rate gradient was applied simultaneously with the organic modifier gradient, allowing us to reach 100% of the modifier. This approach, called unified chromatography, was introduced by Chester [28]. The adjustment of the eluent strength of the modifier up to 100% enabled to widen the polarity range of the analyte set suitable for UHPSFC/MS measurements.

3.2. Screening of water percentage and gradient evaluation with BEH column

The chromatographic performance of the Viridis BEH column was evaluated for three different percentages (1%, 2% and 5%) of water in the methanolic modifier, while the concentration of ammonium acetate was kept constant at 30 mmol L^{-1}. The addition of 2–7% of water to the modifier [12,16,20,31] to facilitate the elution of polar compounds and to improve peak shape, probably caused by the improved solubility, is commonly reported in the recent literature. Six consecutive injections of the standard mixture were performed in positive and negative ion modes to test the influence of 1, 2, and 5% H_2O in the modifier on the chromatographic performance. Retention times of 78 selected metabolites are reported in Table S2. Fig. 2 shows the overlay of chromatograms obtained for three different amounts of water in the modifier for various compounds. Generally, the retention time increased with increasing amount of water in the modifier. For some analytes (Fig. 2A,C), the peak shape worsened, and peak tailing occurred using 5% of water in the modifier. Furthermore, a gradual increase in the system pressure was observed using 5% of water in the modifier, which regularly caused overpressure of the instrument. The experiment was repeated after several weeks to ensure that this observation was not an artefact. The same trend of the gradual increase of the system pressure was observed, which could be caused by solubility issues of the additive in the mobile phase leading to precipitation and column blockage. A good compromise was obtained with 2% or 1% of water in the modifier; all compounds were eluted without any impairment of the Gaussian peak shape (Fig. 2). However, nonpolar triacylglycerols and diacylglycerols were eluted close to the void volume with 1% of water in the modifier. Consequently, 2% of water in the modifier was assessed as the most suitable amount of water in the modifier to achieve the best balance in terms of retention time and peak shape.

The next step of the study was to improve the gradient shape to obtain a good separation of the entire standard mixture as well as good peak shapes. Two gradients were evaluated, gradient A (used for the evaluation of the percentage of water in the modifier) starting from 5% modifier to 75% in 10 min, and gradient B starting from 5% modifier to 70% modifier in 8.5 min. Analytes eluted faster and showed better peak shapes with gradient B (Fig. S3B) compared to gradient A (Fig. S3A). Consequently, gradient B was further used for column screening.

3.3. Column screening and performance evaluation

The choice of stationary phase chemistry, column dimensions, and mobile phase composition is crucial for successful separation. Subsequently, various stationary phases were evaluated for the separation performance of the standard metabolite mixture, such as Diol, 2-PIC, 1-AA, DEA, BEH, CEL 1, HSS C18 SB and HSS T3 (Table 2). All columns are classified as UHPSFC columns (except HSS T3), are produced by the same manufacturer (Waters, Torus, and Viridis columns) and most had the same sub-2 µm particle dimensions as well as column length and diameter, for better comparability (100 × 3.0 mm I.D, 1.7 µm, fully porous hybrid silica) [18,21,31].

The eight stationary phases screened were dedicated UHPSFC columns from the same manufacturer with sub-2 µm particles. The majority of the stationary phases are composed of the same backbone (bridged ethylene hybrid particles) ensuring that the non-selective interactions are comparable and the different selectors bonded on the silica support cause differences in the chromatographic performance. The different selectors bonded to the silica support allow different selectivities for the separation of the studied metabolites as a result of the different interaction capabilities of the analyte and the stationary phase. The simplest stationary phase regarding the selector structure is the BEH column with free silanols on the surface, allowing H-bonding and hydrophilic interactions. For the Diol column, propandiol is linked to the modified silica support. Consequently, the hydroxyl groups allow H-bonding and hydrophilic interactions, but the hydrocarbon chains provide hydrophobic interactions as well. The silica particles of Torus 2-PIC, Torus 1-AA, and Torus DEA are modified with 2-picolyl-amine, 1-amino-anthracene, and diethylamine, respectively. These structures allow multiple interactions of the selector with the analyte, such as steric interactions, hydrogen bonding, Van der Waals interactions, dipole-dipole interactions, anionic exchange type, or π-π interactions. The columns HSS C18 SB (100 × 3 mm I.D; 1.8 µm) and HSS T3 (100 × 2.1 mm I.D; 1.8 µm) columns are packed with silica particles modified with octadecyl bonded ligands on the surface, enabling hydrophobic interactions. The columns differ in their residual activity of the silanol group, as HSS C18 T3 is end-capped compared to HSS C18 SB. The free residual silanol groups additionally

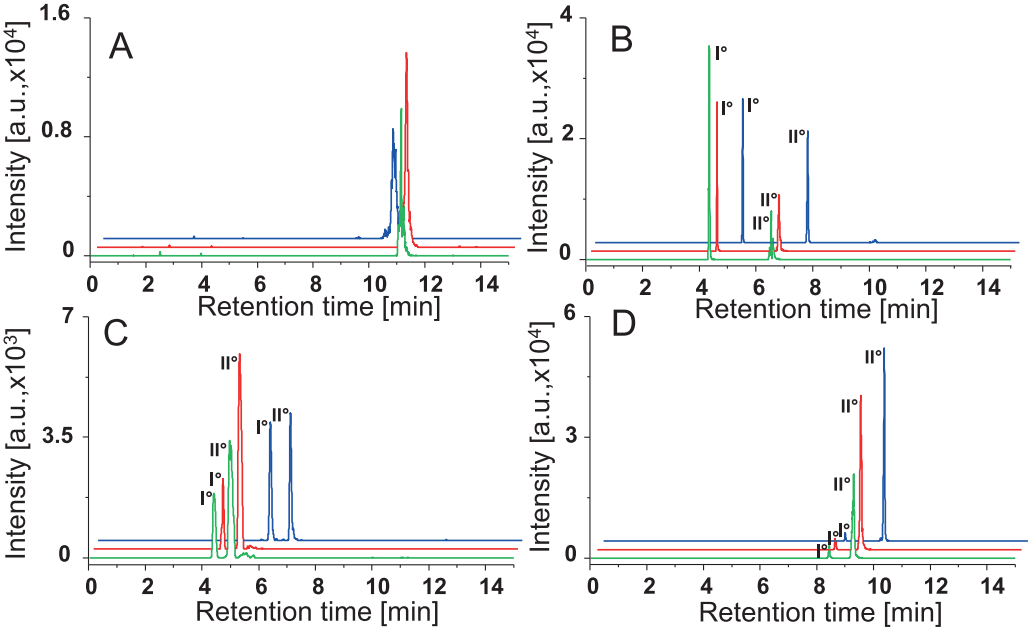

Fig. 2. Effect of water percentage (1% - green, 2% - red, and 5% - blue) in the mobile phase on the retention behavior of selected metabolites: A) L-tryptophan, B) N-acetyl-5-OH-tryptamine (I°) and serotonin (II°), C) D-glucose (I°) and myo-inositol (II°), and D) LPC (18:1) (I°) and PC (36:2) (II°). Analytical conditions: BEH (100 × 3.0 mm, 1.7 µm) column; 60 °C; 1800 psi (ABPR); mobile phase: CH_3OH + 30 mmol L^{-1} ammonium acetate, and 1%, 2%, and 5%; composition of the make-up solvent: CH_3OH + 0.1% formic acid and 5% of H_2O.

allow hydrophilic interactions in the case of the HSS C18 SB, which may be advantageous for the analysis of polar compounds. Trefoil CEL1 (150 × 3.0 mm I.D; 2.5 µm) is a stationary phase based on polysaccharides, in which the silica gel is modified with cellulose tris-(3,5-dimethylphenylcarbamate), allowing multiple interactions such as steric interactions, hydrogen bonding, π-π interactions.

Different chromatographic parameters were evaluated to determine the best column for the separation of the analyte mixture, such as the number of compounds not detected and the peak asymmetry factor (A_s), which is calculated as the ratio of the peak width in the back half and the peak width in the front half at 10% of the peak height. For better comparability, the same gradient was applied for the separation of 78 metabolites for all stationary phases investigated (Fig. S3B). The retention times of each standard for each tested column are reported in Table S2. Fig. 3A shows the chromatograms of guanine and guanosine depending on the employed stationary phase. The highest number of compounds detected, depending on the stationary phase, was as follows: Diol > BEH > 2-PIC > HSS C18 SB > DEA > Cel 1 > 1-AA > HSS T3 (Fig. 3B). This indicates that with increasing hydrophobicity and bulkiness of the stationary phase selector, less analytes are detected. However, some hydrophobic interactions favor separation and detection in comparison to only hydrophilic interactions, as reflected for the Diol and BEH columns. Each compound was injected separately as well as in a mixture for each column. Therefore, the compounds not detected in the analyte mixture are below the detection sensitivity because they were identified when injected separately, some at higher concentrations. This proves that the analytes are eluted for each column, but because of the broad peak shape and high asymmetry, they were below the detection sensitivity, not allowing their identification. The most difficult compounds to identify for most of the columns were metabolites with primary amines in the structure. The primary amines may undergo ionic interactions with the free silanols of the stationary phase. As ionic interactions are generally slow, broad peak shapes can be observed, which may lead to sensitivity issues. The enhancement of the cation concentration in the mobile phase could lead to an improvement of the peak shape and sensitivity since cations function as displacers. On the other hand, increased base concentrations in the mobile phase may lead to ion suppression. The detection sensitivity was diminished especially for the metabolites PS, LPS, PG, LPG, PA and LPA, putrescine, spermine, spermidine, and dopamine, and 5-methoxyindole, 5-hydroxyindole, D,L-kynurenine, and folic acid.

The performance of the column was generally considered acceptable when the A_s value was in the range of 0.9–1.5. Therefore, for each column, the percentage of compounds not detected, the analytes with A_s below 0.9 and with A_s greater than 1.5 were calculated (Fig. S4). The highest percentage of symmetrical peaks was observed for BEH > DEA > Diol > Cel 1 > 1-AA > 2-PIC > HSS C18 > HSS T3 in positive ion mode and BEH > DEA > 2-PIC > HSS T3 > Cel 1 > Diol > 1-AA > HSS C18 in negative ion mode (Table S3). Furthermore, the asymmetry values of each detected compound and their total average for the eight screened columns are reported in Table S3. Broad chromatographic peaks and tailing were found for the lipid classes PS, LPS, PG, LPG, PA, and LPA, as also known from the literature. For biogenic amines, namely spermine, spermidine, and putrescine, a broad and distorted peak shape was observed. The results suggest that the Diol column represents a good compromise between the number of detected peaks and the asymmetry values compared to the other seven columns.

The performance of the method was further investigated by determining the mass accuracy, selectivity, resolution, peak area, peak height, retention time stability, and number of total compounds detected in both polarity modes (Tables S4–S9). L-tryptophan was selected as the reference compound for the calculation of resolution and selectivity, as one of the last eluting analytes. The average time of the first peak in the run from three consecutive blanks (solution of $CH_3OH/CHCl_3$, 1:1 *v/v*) was considered as the void time needed to calculate the capacity factors (Table S5). The median of selectivity and the average of all determined resolution values for each column were investigated. They were determined from the average values of six consecutive injections of the standard mixture for each column by applying the optimized conditions. The median and the average of the overall mass accuracy, selectivity, and resolution are reported in Ta-

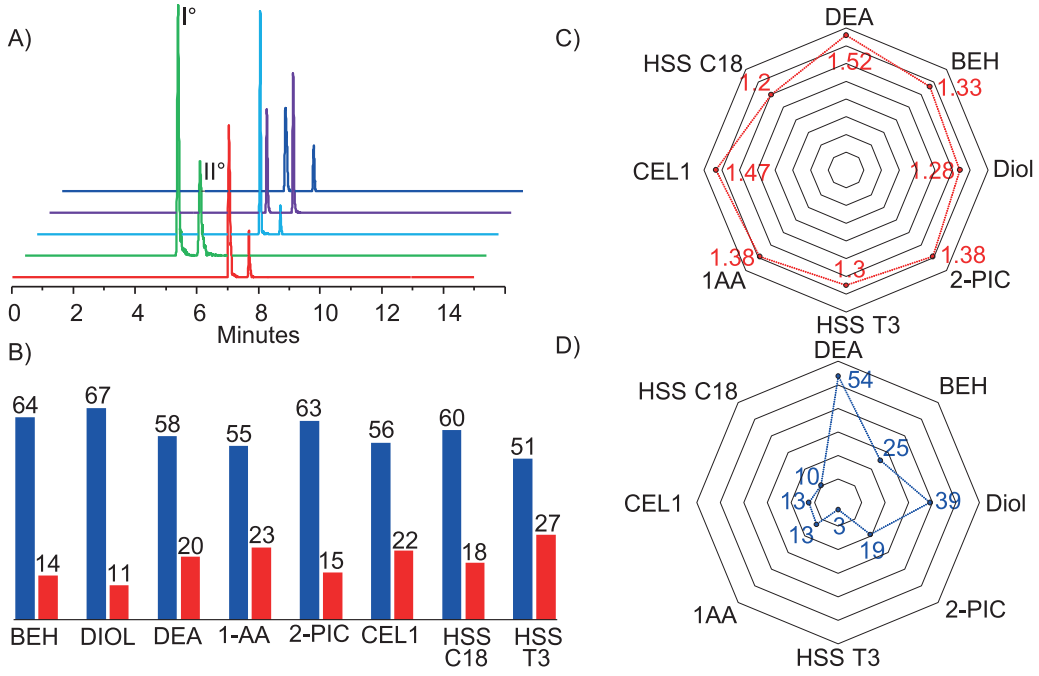

Fig. 3. (A) Selected chromatograms for guanine (I°) and guanosine (II°) on the various stationary phases (red: 1-AA, green: BEH, light blue: Diol, violet: 2-PIC, dark blue: DEA). (B) Bar chart for the number of detected compounds (blue) and non-detected compounds (red) for individual screened columns. (C) Median of the selectivity values and (D) Average of the resolution values for all metabolites on the various stationary phases. Analytical conditions: mobile phase: CH_3OH + 30 mmol L^{-1} ammonium acetate and 2% of water; mobile phase of the make-up pump: CH_3OH + 0.1% formic acid and 5% of H_2O; 60 °C, 1800 psi (ABPR), ESI (+) and ESI (−).

bles S4–S6, as well as the average and RSD% of the peak area, peak height, and retention time in Tables S7–S9. The median obtained for all analytes was used to compare the overall selectivity of the stationary phases, since the overall average may be influenced by analytes eluted close to the void volume. The highest median selectivity was observed for DEA > Cel 1 > 2-PIC = 1-AA > BEH > HSS T3 > Diol > HSS C18 in positive ion (Fig. 3C) mode and BEH > 1-AA > 2-PIC = HSS T3 = HSS C18 > Cel 1 > Diol > DEA in negative ion mode (Table S5). It should be mentioned that much fewer compounds were detected and differences in the median selectivity are negligible in the negative ion mode compared to the positive ion mode (Tables S2 and S5). The highest average resolution was observed for DEA > Diol > BEH > 2-PIC > 1-AA > Cel 1 > HSS C18 > HSS T3 in positive (Fig. 3D) and DEA > Diol > BEH > 2-PIC > 1-AA > HSS C18 > Cel 1 > HSS T3 in negative ion mode (Table S6). A small shift in mass precision was observed, which corresponds to the retention time of the analyte (Table S4). The ionization efficiency depends on the gradient shape of the chromatographic run and, consequently, on the retention times of the analytes. Furthermore, the type of interactions of the analytes with the stationary phase influences the peak shape, because ionic interactions are slow and may lead to broader peaks in comparison to faster interactions such as interactions based on partition or solubility. The peak area, peak height, and average retention time together with the retention time stability were investigated. The highest average peak area was observed for HSS T3 > HSS C18 > Diol > BEH > Cel 1 > 1-AA > 2-PIC > DEA in positive ion mode and HSS T3 > HSS C18 > Cel 1 > > BEH > 2-PIC > Diol > 1-AA > DEA in negative ion mode (Table S7). The highest average peak height was observed for HSS T3 > HSS C18 > 2-PIC > Diol > 1-AA > BEH > Cel 1 > DEA in positive ion mode and Diol > DEA > 2-PIC > BEH > 1-AA > Cel 1 > HSS C18 > HSS T3 in negative ion mode (Table S8). The average retention times on the different stationary phases show the distribution of analytes within the chromatographic run and the extent and type of interactions of the analyte with the selector. The highest average retention time was observed for BEH > HSS C18 > Diol > 1-AA > DEA > 2-PIC > Cel 1 > HSS T3 in positive ion mode and BEH > DEA > Diol > 1-AA > 2-PIC > HSS C18 > Cel 1 > HSS T3 in negative ion mode. The relative standard deviation of the retention times of the analyte for 6 consecutive injections of the metabolite mixture on each stationary phase was investigated, describing the reproducibility of the retention time. The highest stability of retention time was observed for Diol > Cel 1 > DEA > 1-AA > 2-PIC > BEH > HSS C18 > HSS T3 in positive ion mode and DEA > Diol > 1-AA > 2-PIC > BEH > Cel 1 > HSS C18 > HSS T3 in negative ion mode.

The Diol column did not provide the best results for each evaluated parameter, but the comparison of the chromatographic parameters mentioned for each compound and stationary phase, including the total number of detected peaks in positive and negative ion modes, reveals that the overall best performance was achieved with the Diol column, as also previously reported for urinary metabolites [18]. 67 of the 78 structural and chemical highly diverse compounds in the mixture were detected on the Diol column. In order to investigate the reason for detected and non-detected compounds depending on the analyte structure, the analyte set was classified according to their functional groups (Table S14). However, no general trend depending on the presence of functional groups was observed. The Diol column was used for further evaluation within this study. The putative explanation for which Diol worked well for the separation of most of the analytes is the possible polar and hydrophobic interactions of the stationary phase with the polar and hydrophobic parts of the analytes. Further, the small selector structure of the Diol column may favor the accessibility of the analytes to interact with the selector of the stationary phase, in contrast to the bigger selectors tested, which may be leading to steric hindrance.

The reliable separation of isomeric and/or isobaric metabolites in complex biological samples is important in metabolomics studies. Examples of isomeric metabolites included in our selected standard mixture are leucine, isoleucine, and norleucine, some sug-

ars such as D-glucose and myo-inositol, dopamine and octopamine, as well as N-acetyl-serotonin and 1-methyl-tryptophan. Examples of isobaric metabolites investigated are asparagine and ornithine, aspartic acid and 5–hydroxy-indole, glutamine, and lysine, as well as glutamic acid and 5–methoxy-indole. Only the BEH and the Diol column yielded a partial separation of leucine and isoleucine with respect to norleucine, while their coelution with all other columns was detected. Dopamine and octopamine are also important examples of isomers. The first was below its detection sensitivity, which did not allow detection in most cases; on the other hand, octopamine was easily detected. However, each standard was injected individually, allowing good separation between these two compounds. In fact, octopamine was eluted on each column between 5 and 7 min, while dopamine was eluted between 8 and 9 min on various stationary phases. Finally, the isomers D-glucose and myo-inositol, as well as N-acetyl-serotonin and 1-methyl-tryptophan, were always separated independently of the stationary phase. All detected isobaric metabolite pairs were as well separated on all stationary phases investigated. These results have shown that the optimized method provides good separation of not only very diverse metabolites but also some of their isomers and isobars.

18 of the 78 compounds investigated in our study were also included in the analyte set investigated by *Losacco* et al. of 49 compounds [16] and *Desfontaine* et al. of 57 compounds [12], such as some amino acids, biogenic amines, nucleosides and lipids. For comparison reasons, special focus was placed on the evaluation of the separation performance of those compounds. A good peak shape and peak asymmetry have been reached applying the Diol column, i.e., for adenosine, leucine, and sphingomyelin (1.61, 1.45, and 1.31, respectively; Table S3). Additionally, the% RSD of retention time stability was determined for each column (Table S9). The overall stability of the retention time was 0.31% RSD for the Diol column and 0.06, 0.41 and 0.07% for adenosine, leucine and sphingomyelin, respectively. In conclusion, the reported method yielded comparable results for the Diol column in comparison to the data shown by *Losacco* et al. using the Poroshell HILIC column [16]. It is important to emphasize, that the column screening was performed for UHPSFC/MS dedicated sub 2-µm columns from the same manufacturer and the larger set of analytes in terms of polarity and mass range in the present work. The metabolites investigated are mainly interrelated (Figs. S1 and S2), besides chosen analytes included to study mechanistic aspects. This enabled a complete and exhaustive analysis of chromatographic and mass spectrometric parameters.

3.4. Evaluation of ammonium acetate versus ammonium formate as an additive in the modifier

The influence of the type of additive in the mobile phase on retention time, peak area, peak height, mass accuracy, selectivity, resolution, and peak asymmetry for the standard mixture was investigated using the Diol column. Six consecutive injections were performed using 30 mmol L^{-1} of ammonium acetate in CH_3OH/H_2O (98:2, v/v) or 30 mmol L^{-1} of ammonium formate in CH_3OH/H_2O (98:2, v/v) as a modifier. The peak areas and heights of each detected compound were normalized to the average intensity of the lock mass to diminish the influence of the drift of the instrumental response over time (Table S10). The processed data of the normalized area and normalized height were compared using bar graphs for the positive (Figs. S5 and S6) and negative (Figs. S7 and S8) ionization mode. Signal responses for all compounds were higher for ammonium acetate compared to ammonium formate (Table S10). As a result, a higher number of compounds were detected with ammonium acetate (67) than with ammonium formate (65). Table 3 shows a summary of the average

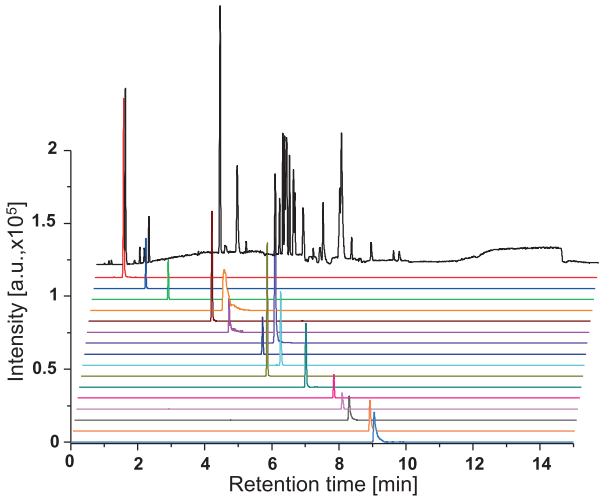

Fig. 4. Base peak intensity chromatograms of the standard set of metabolites obtained under optimized conditions (black) and reconstructed ion current chromatograms for selected compounds: caffeine (red), MG (0:0/18:1/0:0) (blue), Cer (d36:2) (olive), sphinganine (d18:0) (orange), melatonin (wine), adenine (magenta), adenosine (violet), N-acetyl-5-OH-tryptamine (royal), LPC (18:1/0:0) (cyan), palmitoylcarnitine (dark yellow), acetylcarnitine (dark cyan), taurine (pink), L-tyrosine (light magenta), L-tryptophan (dark gray), 5-OH-L-tryptophan (light orange), and L-arginine (light blue). Analytical conditions: Diol (100 × 3.0 mm; 1.7 µm); mobile phase: CH_3OH + 30 mmol L^{-1} ammonium acetate and 2% of water; composition of the make-up solvent: CH_3OH + 0.1% formic acid and 5% of H_2O; 60 °C, 1800 psi (ABPR), ESI (+).

mass accuracy, selectivity, resolution and RSD of the peak area, peak height, and retention time. Furthermore, detailed values for each compound, depending on the additive applied on the Diol column, are reported in Tables S3–S10 for ammonium acetate and Tables S10–S11 for ammonium formate. The average mass accuracy, selectivity, and resolution was slightly higher for ammonium formate than ammonium acetate (Table 3). No general trend was observed for the signal and retention time stability depending on the additive. However, ammonium acetate was selected as the additive of choice in the mobile phase for the investigated analyte set because of the slightly higher number of detected compounds and the higher signal response. Data processing was performed independently with TargetLynx, which was used by default, and MZmine, to assess whether the data processing software has an impact on the results (Table S11). The same chromatographic and method parameters were investigated with MZmine as with TargetLynx, and compared to each other. Data were comparable but not the same, which shows that the data processing software employed may have an impact on the results.

Finally, the Diol column (100 × 3 mm I.D; 1.7 µm), the modifier of MeOH with 30 mmol L^{-1} ammonium acetate and 2% of water, the make-up solvent of MeOH with 0.1% formic acid and 5% of water (see Fig. 4) were evaluated as the best choice for the separation of the investigated analyte set.

3.5. Comparison of ESI and APCI ionization techniques

The ionization efficiency may change depending on the chemical properties and chemical structure of the analyzed compounds and the applied ion source. ESI is the most widely used ion source. Sensitivity strongly depends on the flow rates employed, since ESI represents a concentration-dependent ionization technique. APCI is a mass flow dependent ionization process more suitable for higher flow rates. UHPSFC/MS methods generally use flow rates higher than those of UHPLC/MS methods; therefore, the evaluation of the ion source on the ionization efficiency of target compounds may be of interest. However, the majority of UHPSFC/MS methods use

a splitter, which reduces the flow into the mass spectrometer favoring ESI. A systematic investigation was conducted to evaluate the influence of the ionization source on the number and type of detected analytes. The standard mixture was analyzed by ESI and APCI in both polarity modes. The optimized chromatographic conditions and optimized ion source parameters were applied. The results showed that ESI in general led to a higher ionization efficiency compared to APCI (Figs. S9–S12). However, for some analytes, the peak area and peak height (normalized to the sum area and sum height considering the total compounds in the positive and negative ionization mode for the ESI and APCI sources) were higher for the APCI source than for the ESI source, showing that ESI and APCI can be complementary (Table S12). The sensitivity was higher for several amino acids, such as L-tyrosine, ornithine, phenylalanine, taurine, as well as L-tryptophan, L-arginine, and L-lysine and two nucleosides (adenine and guanine) using APCI, and dopamine was only detected using the APCI source. On the other hand, the areas and heights of the L-carnitine derivatives, LPC (18:0), and melatonin were enhanced with ESI. L-carnitine and acetyl-L-carnitine were only detected using ESI. To illustrate the comparison of the normalized area and height for some identified standards in positive ion mode for both ion sources, bar graphs are shown in Figs. S9–S12. The corresponding values of the normalized peak areas, heights, and retention times of each standard for both ion sources are reported in Table S12. The total number of detected compounds was 67 and 48 for ESI and APCI, respectively, showing the wider application range of ESI for the investigated analyte set [32]. In the negative ionization mode, most analytes were not detected using APCI (Figs. S11 and S12). Furthermore, in the negative ionization mode, the signal response was significantly lower than in the positive ionization mode, regardless of the ion source type. ESI provided the overall best ionization efficiency for the analyte set in both ion modes.

3.6. Application to human plasma

Optimized chromatographic and MS conditions were applied for the analysis of pooled human plasma samples to evaluate the applicability of the method to real samples. The protocol used for sample preparation was based on the application of an additional step prior to protein precipitation based on the addition of proteinase K. This procedure allowed the release of associated metabolites through relaxation of the tertiary structure of native proteins and consequently a higher possibility of their identification [41]. In addition, plasma samples obtained by the following protein precipitation were injected and analyzed in MS^E mode. MS^E mode allows the untargeted scanning of the MS and MS/MS levels by applying low and high collision energy within one run. This increases the identification confidence of metabolites, as the characteristic fragments of metabolites provide additional information. First, the standard mixture was analyzed to obtain clean fragment ion spectra as reference without interferences caused by the complex matrix of a real human plasma sample using ESI and APCI. No differences in fragmentation behavior were observed between ESI and APCI (Table S13). The diluted human plasma sample (1:10) was analyzed using ESI and APCI. Fig. 5A shows the TIC of human plasma obtained with ESI and APCI. It can be seen that the sensitivity is higher for ESI than APCI, also for real human plasma samples. The extracted ion chromatograms (XIC) of selected metabolites detected in human plasma are presented in Fig. 5B using ESI. The targeted data analysis revealed that 44 and 5 compounds included in the analyte set were also detected in the diluted plasma sample using ESI and APCI, respectively, in positive and negative ion mode (Table S15). The reduction of the sample complexity by optimizing the sample preparation protocol, i.e., using solid phase extraction, may help increasing the sensitivity to detect the whole analyte set in human plasma. The untargeted MS^E approach allowed the use of metabolomics databases to link *m/z* features to

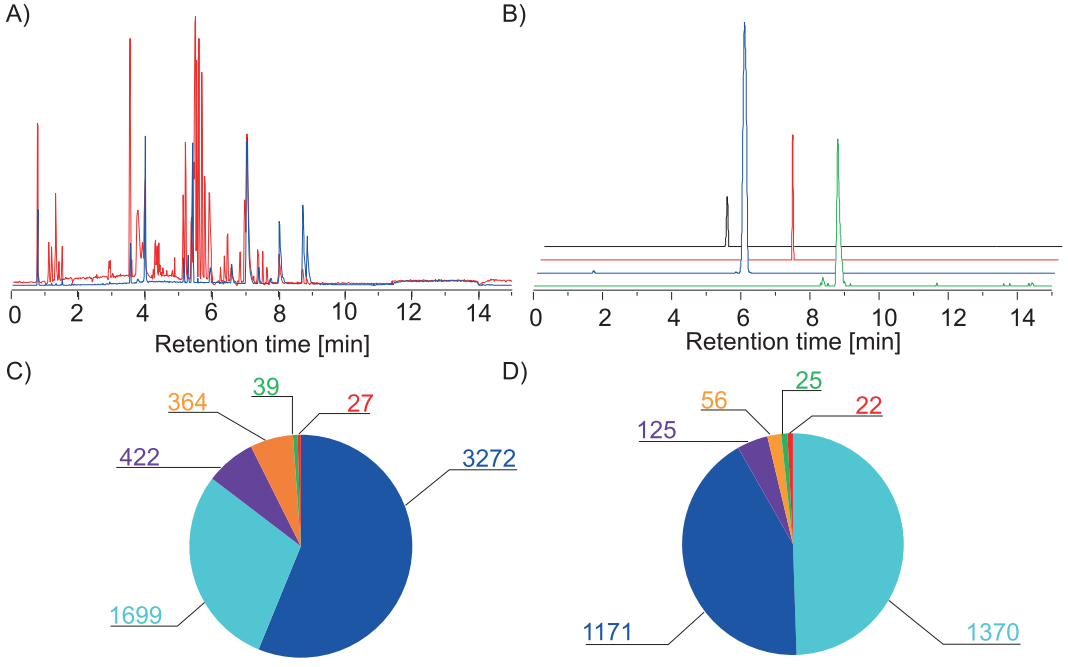

Fig. 5. (A) Impact of the type of ion source on sensitivity. Base peak intensity chromatogram of human plasma using red) ESI and blue) APCI. (B) Selected extracted ion chromatograms of human plasma using ESI (green: ornithine, blue: glucose, red: serotonine, black: adenosine) Pie charts of the untargeted *m/z* feature analysis in human plasma for (C) positive and (D) negative ion mode using MS DIAL. 5823 *m/z* features were detected in positive and 2769 *m/z* features in negative ion mode. The *m/z* features were categorized according to the compound class: red) analyte set of the study, green) nucleoside and derivatives, orange) amino acids and derivatives, violet) polyphenols, light blue) lipids and dark blue) other metabolites. Analytical conditions: Diol (100 × 3.0 mm; 1.7 µm); mobile phase: CH_3OH + 30 mmol L^{-1} ammonium acetate and 2% of water; composition of the make-up solvent: CH_3OH + 0.1% formic acid and 5% of H_2O; 60 °C, 1800 psi (ABPR), ESI (+).

metabolites for identification. MSDIAL was used for the identification of metabolites considering also the MS2 level. The optimized method allowed the detection of 5823 and 2789 features in human plasma in positive and negative ion mode, respectively, using ESI (Fig. 5C,D). The detected features were classified according to the compound class, such as amino acids and derivatives, nucleosides and derivatives, polyphenols, lipids, other metabolites, and compounds included in the analyte set. The 27 and 22 compounds also included in the analyte set for optimization detected with MSDIAL in positive and negative ion mode, were also identified with TargetLynx when targeted data processing was applied. Generally, a few more compounds belonging to the analyte set were identified with TargetLynx (38 and 23 compounds in positive and negative ion mode) than MSDIAL, due to the optimized filtering and threshold settings applied for MSDIAL. This, together with the comparison of the MS2 spectra and the retention times of all compounds present in the standard mixture to the real sample, allowed a certain quality control, may minimizing the risk of overreporting of identified compounds by MSDIAL.

4. Conclusion

The goal of this work was the development of a UHPSFC/MS method for the qualitative analysis of a wide range of metabolites in terms of polarity and its application to human plasma samples. Particular attention was paid to the choice of the optimal chromatographic column and the mobile phase composition. The set of 78 standards was chosen for the evaluation of chromatographic parameters, allowing the standard mixture to represent plasma metabolites that are interrelated and of clinical relevance. Preliminary tests were performed on the Viridis BEH column and subsequently optimized conditions were applied for the screening of eight dedicated UHPSFC/MS columns from the same manufacturer ensuring comparable non-selective interactions from the particle backbone. The best column for the separation of the standard mixture was the Torus Diol column with 67 out of 78 detected compounds with selectivity and resolution values of 1.28 and 39, respectively. Furthermore, the optimized method allowed the separation of important metabolite isomers, such as myo-inositol and D-glucose, as well as amino acids L-leucine, L-isoleucine, and L-norleucine. The sensitivity was higher for ammonium acetate compared to ammonium formate used as an additive in the modifier. Data processing was performed with two different software packages, TargetLynx and MZmine. The results were comparable but not the same, highlighting the importance of experimental details in untargeted metabolomics. Finally, the influence of ESI and APCI ion sources on the ionization efficiency was evaluated for the standard mixture and human plasma samples using MS^E mode. Generally, ESI provides higher sensitivity in comparison to APCI. The applicability of UHPSFC/MS for the qualitative metabolomic analysis has been confirmed, but there is still a need for further improvements, such as the optimization of the sample preparation protocol, to obtain a sensitive, quantitative method using UHPSFC/MS.

Declaration of Competing Interest

The authors declare that they have no conflict of interest.

CRediT authorship contribution statement

Michela Antonelli: Investigation, Formal analysis, Writing – original draft, Visualization. **Michal Holčapek:** Resources, Writing – review & editing. **Denise Wolrab:** Conceptualization, Funding acquisition, Supervision, Project administration, Writing – review & editing.

Acknowledgment

This work was supported by the junior grant project 20-23290Y funded by the Czech Science Foundation. M.A. acknowledges the support of the project “International mobility of employees of the University of Pardubice II” CZ.02.2.69/0.0/0.0/18_053/0016969.

Supplementary materials

Supplementary material associated with this article can be found, in the online version, at doi:10.1016/j.ejps.2020.105216.

References

[1] C. Gieger, L. Geistlinger, E. Altmaier, M.H. De Angelis, F. Kronenberg, T. Meitinger, H.W. Mewes, H.E. Wichmann, K.M. Weinberger, J. Adamski, T. Illig, K. Suhre, Genetics meets metabolomics: a genome-wide association study of metabolite profiles in human serum, PLoS Genet. 4 (2008), doi:10.1371/journal.pgen.1000282.
[2] Y. Chen, J. Xu, R. Zhang, Z. Abliz, Methods used to increase the comprehensive coverage of urinary and plasma metabolomes by MS, Bioanalysis 8 (2016) 981–997, doi:10.4155/bio-2015-0010.
[3] U. Roessner, J. Bowne, What is metabolomics all about? BioTechniques 46 (2009) 363–365, doi:10.2144/000113133.
[4] I. Kohler, M. Giera, Recent advances in liquid-phase separations for clinical metabolomics, J. Sep. Sci. 40 (2017) 93–108, doi:10.1002/jssc.201600981.
[5] M. Zhou, L. Song, S. Ye, W. Zeng, H. Hännien, W. Yu, J. Suo, Y. Hu, J. Wu, New sights into lipid metabolism regulation by low temperature in harvested Torreya grandis nuts, J. Sci. Food Agric. 99 (2019) 4226–4234, doi:10.1002/jsfa.9653.
[6] W.B. Dunn, D. Broadhurst, P. Begley, E. Zelena, S. Francis-Mcintyre, N. Anderson, M. Brown, J.D. Knowles, A. Halsall, J.N. Haselden, A.W. Nicholls, I.D. Wilson, D.B. Kell, R. Goodacre, Procedures for large-scale metabolic profiling of serum and plasma using gas chromatography and liquid chromatography coupled to mass spectrometry, Nat. Protoc. 6 (2011) 1060–1083, doi:10.1038/nprot.2011.335.
[7] E. Zelena, W.B. Dunn, D. Broadhurst, S. Francis-McIntyre, K.M. Carroll, P. Begley, S. O'Hagan, J.D. Knowles, A. Halsall, I.D. Wilson, D.B. Kell, Development of a robust and repeatable UPLC - MS method for the long-term metabolomic study of human serum, Anal. Chem. 81 (2009) 1357–1364, doi:10.1021/ac8019366.
[8] H.G. Gika, G.A. Theodoridis, R.S. Plumb, I.D. Wilson, Current practice of liquid chromatography-mass spectrometry in metabolomics and metabonomics, J. Pharm. Biomed. Anal. 87 (2014) 12–25, doi:10.1016/j.jpba.2013.06.032.
[9] M.R. Gama, R.G. da Costa Silva, C.H. Collins, C.B.G. Bottoli, Hydrophilic interaction chromatography, TrAC Trends Anal. Chem. (2012) 48–60, doi:10.1016/j.trac.2012.03.009.
[10] B. Buszewski, S. Noga, Hydrophilic interaction liquid chromatography (HILIC)-a powerful separation technique, Anal. Bioanal. Chem. 402 (2012) 231–247, doi:10.1007/s00216-011-5308-5.
[11] C.F. Poole, Stationary phases for packed-column supercritical fluid chromatography, J. Chromatogr. A 1250 (2012) 157–171, doi:10.1016/j.chroma.2011.12.040.
[12] V. Desfontaine, G.L. Losacco, Y. Gagnebin, J. Pezzatti, W.P. Farrell, V. González-Ruiz, S. Rudaz, J.L. Veuthey, D. Guillarme, Applicability of supercritical fluid chromatography – mass spectrometry to metabolomics. I – optimization of separation conditions for the simultaneous analysis of hydrophilic and lipophilic substances, J. Chromatogr. A 1562 (2018) 96–107, doi:10.1016/j.chroma.2018.05.055.
[13] D.A. Klesper, Corwin E, Turner A.H, High pressure gas chromatography above critical temperature, J. Org. Chem. 27 (1962) 700–706, doi:10.1021/jo01049a069.
[14] L. Laboureur, M. Ollero, D. Touboul, Lipidomics by supercritical fluid chromatography, Int. J. Mol. Sci. 16 (2015) 13868–13884, doi:10.3390/ijms160613868.
[15] T. Bamba, J.W. Lee, A. Matsubara, E. Fukusaki, Metabolic profiling of lipids by supercritical fluid chromatography/mass spectrometry, J. Chromatogr. A 1250 (2012) 212–219, doi:10.1016/j.chroma.2012.05.068.
[16] G.L. Losacco, O. Ismail, J. Pezzatti, V. González-Ruiz, J. Boccard, S. Rudaz, J.L. Veuthey, D. Guillarme, Applicability of supercritical fluid chromatography–mass spectrometry to metabolomics. II–assessment of a comprehensive library of metabolites and evaluation of biological matrices, J. Chromatogr. A 1620 (2020) 461021, doi:10.1016/j.chroma.2020.461021.
[17] V. Shulaev, G. Isaac, Supercritical fluid chromatography coupled to mass spectrometry – a metabolomics perspective, J. Chromatogr. B Anal. Technol. Biomed. Life Sci. 1092 (2018) 499–505, doi:10.1016/j.jchromb.2018.06.021.
[18] A. Sen, C. Knappy, M.R. Lewis, R.S. Plumb, I.D. Wilson, J.K. Nicholson, N.W. Smith, Analysis of polar urinary metabolites for metabolic phenotyping using supercritical fluid chromatography and mass spectrometry, J. Chromatogr. A 1449 (2016) 141–155, doi:10.1016/j.chroma.2016.04.040.
[19] W. Zou, J.G. Dorsey, T.L. Chester, Modifier effects on column efficiency in packed-column supercritical fluid chromatography, Anal. Chem. 72 (2000) 3620–3626, doi:10.1021/ac991417u.

[20] A. Raimbault, M. Dorebska, C. West, A chiral unified chromatography–mass spectrometry method to analyze free amino acids, Anal. Bioanal. Chem. 411 (2019) 4909–4917, doi:10.1007/s00216-019-01783-5.
[21] E. Lemasson, S. Bertin, P. Hennig, H. Boiteux, E.L. Westa, C. West, Development of an achiral supercritical fluid chromatography method with ultraviolet absorbance and mass spectrometric detection for impurity profiling of drug candidates. Part I: optimization of mobile phase composition, J. Chromatogr. A 1408 (2015) 217–226, doi:10.1016/j.chroma.2015.07.037.
[22] K. Taguchi, E. Fukusaki, T. Bamba, Supercritical fluid chromatography/mass spectrometry in metabolite analysis, Bioanalysis 6 (2014) 1679–1689, doi:10.4155/bio.14.120.
[23] T.A. Berger, Demonstration of high speeds with low pressure drops using 1.8 μm particles in SFC, Chromatographia 72 (2010) 597–602, doi:10.1365/s10337-010-1699-2.
[24] C. Sarazin, D. Thiébaut, P. Sassiat, J. Vial, Feasibility of ultra high performance supercritical neat carbon dioxide chromatography at conventional pressures, J. Sep. Sci. 34 (2011) 2773–2778, doi:10.1002/jssc.201100332.
[25] A. Grand-Guillaume Perrenoud, J.L. Veuthey, D. Guillarme, The use of columns packed with sub-2 μm particles in supercritical fluid chromatography, TrAC Trends Anal. Chem. 63 (2014) 44–54, doi:10.1016/j.trac.2014.06.023.
[26] C. West, E. Lemasson, S. Bertin, P. Hennig, E. Lesellier, An improved classification of stationary phases for ultra-high performance supercritical fluid chromatography, J. Chromatogr. A 1440 (2016) 212–228, doi:10.1016/j.chroma.2016.02.052.
[27] J. Prothmann, M. Sun, P. Spégel, M. Sandahl, C. Turner, Ultra-high-performance supercritical fluid chromatography with quadrupole-time-of-flight mass spectrometry (UHPSFC/QTOF-MS) for analysis of lignin-derived monomeric compounds in processed lignin samples, Anal. Bioanal. Chem. 409 (2017) 7049–7061, doi:10.1007/s00216-017-0663-5.
[28] T.L. Chester, Chromatography from the mobile-phase perspective, Anal. Chem. 69 (1997) 165A–169A, doi:10.1021/ac971559t.
[29] D. Wolrab, M. Chocholoušková, R. Jirásko, O. Peterka, M. Holčapek, Validation of lipidomic analysis of human plasma and serum by supercritical fluid chromatography–mass spectrometry and hydrophilic interaction liquid chromatography–mass spectrometry, Anal. Bioanal. Chem. 412 (2020) 2375–2388, doi:10.1007/s00216-020-02473-3.
[30] D. Wolrab, M. Chocholoušková, R. Jirásko, O. Peterka, V. Mužáková, H. Študentová, B. Melichar, M. Holčapek, Determination of one year stability of lipid plasma profile and comparison of blood collection tubes using UHPSFC/MS and HILIC-UHPLC/MS, Anal. Chim. Acta 1137 (2020) 74–84, doi:10.1016/j.aca.2020.08.061.
[31] G.L. Losacco, E. Marconetto, R. Nicoli, T. Kuuranne, J. Boccard, S. Rudaz, J.L. Veuthey, D. Guillarme, Supercritical fluid chromatography–mass spectrometry in routine anti-doping analyzes: estimation of retention time variability under reproducible conditions, J. Chromatogr. A 460780 (2020) 1616, doi:10.1016/j.chroma.2019.460780.
[32] D. Wolrab, P. Frühauf, C. Gerner, Direct coupling of supercritical fluid chromatography with tandem mass spectrometry for the analysis of amino acids and related compounds: comparing electrospray ionization and atmospheric pressure chemical ionization, Anal. Chim. Acta 981 (2017) 106–115, doi:10.1016/j.aca.2017.05.005.
[33] C. West, Current trends in supercritical fluid chromatography, Anal. Bioanal. Chem. 410 (2018) 6441–6457, doi:10.1007/s00216-018-1267-4.
[34] T. Pluskal, S. Castillo, A. Villar-Briones, M. Orešič, M. Zmine, 2: modular framework for processing, visualizing, and analyzing mass spectrometry-based molecular profile data, BMC Bioinform. 11 (2010), doi:10.1186/1471-2105-11-395.
[35] X. han Liu, X. yue Zhai, Role of tryptophan metabolism in cancers and therapeutic implications, Biochimie 182 (2021) 131–139, doi:10.1016/j.biochi.2021.01.005.
[36] Z. Galla, C. Rajda, G. Rácz, N. Grecsó, Á. Baráth, L. Vécsei, C. Bereczki, P. Monostori, Simultaneous determination of 30 neurologically and metabolically important molecules: a sensitive and selective way to measure tyrosine and tryptophan pathway metabolites and other biomarkers in human serum and cerebrospinal fluid, J. Chromatogr. A 1635 (2021) 461775, doi:10.1016/j.chroma.2020.461775.
[37] P.B. Ancey, C. Contat, E. Meylan, Glucose transporters in cancer – from tumor cells to the tumor microenvironment, FEBS J. 285 (2018) 2926–2943, doi:10.1111/febs.14577.
[38] W.Y. Hsu, W.T.L. Chen, W. De Lin, F.J. Tsai, Y. Tsai, C.T. Lin, W.Y. Lo, L. Bin Jeng, C.C. Lai, Analysis of urinary nucleosides as potential tumor markers in human colorectal cancer by high performance liquid chromatography/electrospray ionization tandem mass spectrometry, Clin. Chim. Acta 402 (2009) 31–37, doi:10.1016/j.cca.2008.12.009.
[39] D. Wolrab, R. Jirásko, E. Cífková, M. Höring, D. Mei, M. Chocholoušková, O. Peterka, J. Idkowiak, T. Hrnčiarová, L. Kuchař, R. Ahrends, R. Brumarová, D. Friedecký, G. Vivo-Truyols, P. Škrha, J. Škrha, R. Kučera, B. Melichar, G. Liebisch, R. Burkhardt, M.R. Wenk, A. Cazenave-Gassiot, P. Karásek, I. Novotný, K. Greplová, R. Hrstka, M. Holčapek, Lipidomic profiling of human serum enables detection of pancreatic cancer, Nat. Com. 13 (2021) 124, doi:10.1038/s41467-021-27765-9.
[40] G. Bin Lee, J.C. Lee, M.H. Moon, Plasma lipid profile comparison of five different cancers by nanoflow ultrahigh performance liquid chromatography-tandem mass spectrometry, Anal. Chim. Acta 1063 (2019) 117–126, doi:10.1016/j.aca.2019.02.021.
[41] R. Wawrzyniak, A. Kosnowska, S. Macioszek, R. Bartoszewski, M.J. Markuszewski, New plasma preparation approach to enrich metabolome coverage in untargeted metabolomics: plasma protein bound hydrophobic metabolite release with proteinase K, Sci. Rep. 8 (2018) 1–10, doi:10.1038/s41598-018-27983-0.